r = radial distance from center of whole annular configuration to point of measurement in fluid, ft.

r_1 = radius of inner surface, or core, of annulus, ft.

r_2 = radius of outer surface of annulus, ft.

r_m = radius of maximum local fluid velocity, ft.

u = mean local fluid velocity, ft./sec.

u_m = maximum value of mean local fluid velocity, ft./sec.

V = bulk average linear fluid velocity, ft./sec.

Greek Letters

μ = viscosity of fluid, lb.-mass/(sec.)(ft.)

ρ = density of fluid, lb.-mass/cu. ft.

τ_1 = skin friction at inner surface of annulus, lb.-force/sq. ft.

τ_2 = skin friction at outer surface of annulus, lb.-force/sq. ft.

LITERATURE CITED

1. Knudsen, J. G., and D. L. Katz, "Proc. Midwestern Conf. Fluid Dynamics, 1st Conf.," No. 2, 175 (1950).
2. Prengle, R. S., and R. R. Rothfus, *Ind. Eng. Chem.*, **47**, 379 (1955).
3. Rothfus, R. R., C. C. Monrad, and V. E. Senecal, *ibid.*, **42**, 2511 (1950).
4. Rothfus, R. R., C. C. Monrad, K. G. Sikchi, and W. J. Heideger, *ibid.*, **47**, 913 (1955).
5. Rothfus, R. R., J. E. Walker, and G. A. Whan, *A.I.Ch.E. Journal*, **4**, 2 (1958).
6. Stanton, T. E., D. Marshall, and C. N. Bryant, *Proc. Roy. Soc. (London)*, **A97**, 413 (1920).
7. Walker, J. E., G. A. Whan, and R. R. Rothfus, *A.I.Ch.E. Journal*, **3**, (1957).

Manuscript received March 26, 1958; revision received July 3, 1958; paper accepted July 7, 1958.

Some Effects of Baffles on a Fluidized System

R. H. OVERCASHIER, D. B. TODD, and R. B. OLNEY

Shell Development Company, Emeryville, California

Some characteristics are reported for the fluidization of an air-microspheroidal catalyst system in a 16-in.-diameter bed equipped with baffles. The back-mixing characteristics and retention-time distributions of gas and solids, allowable gas and solids velocities, entrainment rate, and bed density are studied as functions of baffle design.

It is shown that the use of baffles narrows the retention-time spectrum and permits either concurrent or countercurrent flow while not seriously reducing gas or solids throughput or solids holdup.

For many reactions a fluidized-bed system offers important advantages, such as uniform temperatures under conditions of high heat release, large surface-to-volume ratio of the solids medium, and ease of transfer of the solids from one process vessel to another. The principal disadvantage of the fluid bed is its broad spectrum of gas and solids holding times. It has been shown that the residence-time spectrum of the fluid bed is much closer to that of a single well-mixed stage than to the more desirable infinite stages (piston flow). As reactor volume and the formation of unwanted by-products via consecutive reactions are both minimized by piston flow, this disadvantage can be serious.

The broad residence-time distribution of the conventional fluidized bed is well established. Singer, Todd, and Guinn (*5*) have shown that for the solids residence times used in commercial catalytic cracking (*5 to 40 min.*) the catalyst in each vessel could be regarded as perfectly mixed. The gas-retention-time studies of Gilliland, Mason, and Oliver (*2, 3*) in small columns showed that while the gas phase appeared neither well mixed nor in piston flow, it was much closer to the former. The present authors' measurements, shown in Figure 1 for a 16-in.-diam. fluid bed, confirm these previous findings. Gilliland, Mason, and Oliver postulated that the gas effluent from the bed results from the combination of two internal streams, one flowing slowly through the interstices of the solid and the other flowing rapidly via large bubbles or cavities containing very little solids. According to this analysis the majority of the gas travels via the rapidly moving bubbles and exchanges incompletely with the interstitial gas (that is, partially by-passes the bed). The resulting system effluent has a retention-time curve approximating the broad spectrum of a well-mixed stage. Similar findings are also reported by Handlos, Kunstman, and Schissler (*4*) for commercial fluidized beds.

If this analysis is correct, the bubbles play an important role in bed dynamics, providing both the density gradient which mixes the solids and the rapid escape path for part of the gas. They also appear inherent in the fluid bed, since they have been observed in many investigations, and their inevitability has been shown recently on theoretical grounds by Baron and Mugele (*1*). Thus the goal of narrowing the residence-time spectrum of the fluid bed appears to rest on minimizing the effect of the bubbles rather than on their elimination.

Many workers in the field of fluidization have suggested compartmenting the bed with horizontal baffles to narrow the residence-time spectrum. These baffles should narrow the spectrum by decreasing the velocity difference between the bubble and interstitial flows and by promoting transfer between them. In addition the baffles should impede the complete mixing of solids and result in staging of the solids flow, either for concurrent or countercurrent flow of solids and gas. Finally, since bubbles would still be present, the individual compartments would still have good heat-transfer characteristics.

The purpose of this investigation is to show the effect of horizontal baffles on the residence-time spectrum of solids and gas and on other characteristics of the fluid bed, such as allowable flow rates, mixture density, and solids entrainment. The experimental apparatus, operating techniques, and calculation

TABLE 1. BAFFLE CONSTRUCTION

Baffle type	Free area %	Openings Size	Openings Number	Baffle thickness, in.	Baffle spacing, in.	No. of baffles
Grid trays	15	¼ in. slots	11	⅛	24	4
	30	¼ in. slots	22	⅛	8, 24	12, 4
	30	1 in. slots	5	⅛, 1	24	4
Tube trays	2.4	1.5 in. tubes	3	6	42	2
	4.6	2.0 in. tubes	3	6	42	2
	9.2	2.0 in. tubes	6	6	42	2
	4.7	1 in. tubes	12	1, 3	27	4
	14.5	1 in. tubes	37	3	27	4

TABLE 2. CATALYST PROPERTIES

Surface area	90 sq. meters/g.
Pore volume	0.23 cc./g.
Skeletal density	2.3 g./cc.
Particle density	1.5 g./cc.
Size distribution*	
D_{10}	51 μ
D_{50}	77 μ
D_{90}	103 μ

*D_{10}, D_{50}, and D_{90} are the particle diameters corresponding to 10, 50, and 90% respectively of the cumulative weight distribution, as determined by Micromerograph analysis.

methods are described in the following sections.

APPARATUS

All the measurements were made in the system diagrammed in Figure 2. The fluid bed was contained in a plastic column, 16 in. in diameter by 10 ft. high. Humidified air was metered through a standard A.S.M.E. long-radius approach nozzle and flowed up through the dense bed. Separation of the air and solids took place initially in the disengaging section above the fluid bed and finally in a two-stage cyclone system.

For concurrent flow, solids were entrained up the column and returned to the bottom of the bed continuously via the standpipe of the primary cyclone and intermittently from the secondary cyclone. The external solids circulation rate was dependent upon the gas velocity and the inventory of solids contained in the system.

For countercurrent flow a large-diameter disengaging space was provided at the top of the column. Solids were withdrawn from the bottom of the bed and transported to the top of the bed through a calibrated dilute-phase riser. The solids circulation rate was controlled by a butterfly valve at the bottom of the column. The entrained solids were returned to the top of the bed directly from the cyclone standpipes. The solids entrainment rate to the cyclones was estimated from the air flow and pressure drop through a calibrated nozzle placed in the column exit line.

Helium and Freon, used as tracers in both steady and unsteady state gas experiments, were analyzed in a thermal conductivity apparatus. The analyzer required about 300 cc. of gas and 3 min. for each determination. Gas samples were withdrawn into brine-trapped bottles via assemblies containing six fritted-glass filters arranged along a column diameter. These assemblies could be installed at 4-in. intervals up the column. In the back-mixing experiment (steady state) the sample was withdrawn slowly over a long period (~5 min.) to ensure sampling the interstices rather than the rising bubbles. In the by-passing experiments the samples were withdrawn quickly (300 cc. in about 1 sec.) at a point far enough above the dense bed to assure mixing of both the bubble and interstitial gas. Samples taken at varying heights above the dense bed were related by assuming plug flow in the dilute zone after this practice was shown experimentally to be justified.

The types of baffles investigated are depicted in Figure 2 and described in detail in Table 1. All the trays studied were without downcomers; that is, both the gas and solids passed through the same openings. The number of compartments in operation during any one run depended upon the total solids inventory. Occasionally there was no dense phase above the top baffle.

CATALYST PROPERTIES

In all the tests the fluidized solids were equilibrium, microspheroidal, silica-alumina, cracking catalyst which had been regenerated to whiteness. The catalyst had the average properties given in Table 2 with an incipient fluidization velocity of less than 0.01 ft./sec.

INTERPRETIVE MODELS

The change in gas- and solids-residence-time distributions brought about by the use of baffles was investigated by studying the outlet response to step or pulse input functions.

For the gas studies both transient retention time and steady state back-mixing experiments were performed. The retention-time data were compared with theoretical curves calculated for several models suggested by observation of a fluidized bed. These models are

1. Perfect mixing in each stage
2. Perfect mixing within each stage but with a fraction of the gas by-passing the stage at infinite velocity and subsequently mixing with the unby-passed fraction
3. Perfect mixing in which the by-passed gas fraction travels at some finite velocity
4. Mass transfer occurring between a plug-flow bubble phase and a well-mixed interstitial gas phase, with the gas entering and leaving the system via the bubble phase, which travels at some finite velocity
5. Mass transfer occurring between a well-mixed bubble phase and a well-mixed interstitial phase with gas entering and leaving via the bubbles, which travel at some finite velocity

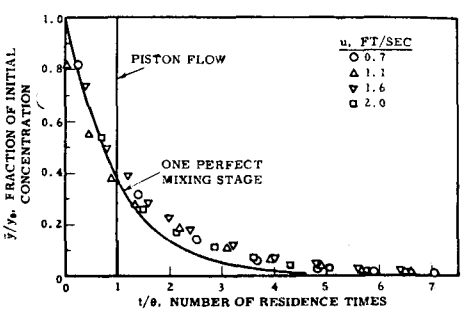

Fig. 1. Gas retention time in a 16-in. diameter unbaffled bed.

Since the experimental curves were not precisely fitted by any of the models, the experiments were interpreted primarily on the basis of the width of the residence-time spectrum. For this reason the models are described here superficially and in more detail in the supplement.*

For perfect mixers without by-passing, the time-concentration history of the effluent is given by

$$y_1/y_0 = \exp(-t/\theta) \qquad (1)$$

for a single stage and

$$y_n/y_0 = \exp\left(-\frac{t}{\theta}\right)\sum_{p=0}^{n-1}\frac{1}{p!}\left(\frac{t}{\theta}\right)^p \qquad (2)$$

for n identical stages in series.

For perfect mixers with infinite-velocity by-passing of a fraction $(1-\epsilon)$ around each stage and with remixing of the fractions $(1-\epsilon)$ and ϵ between stages

$$\bar{y}_1/y_0 = \epsilon\exp\left(-\epsilon\frac{t}{\theta}\right) \qquad (3)$$

for a single stage, and

$$\bar{y}_n/y_0 = \epsilon\exp\left(-\epsilon\frac{t}{\theta}\right)\sum_{p=0}^{n-1}c_p\frac{\epsilon^{2p}}{p!}\left(\frac{t}{\theta}\right)^p \qquad (4)$$

for n identical stages in series, where

$$c_0 = \frac{1-(1-\epsilon)^n}{\epsilon}$$

$$c_{p+1} = -\frac{1}{p+1}\frac{dc_p}{d\epsilon}$$

For finite-velocity by-passing in a single stage

$$\bar{y}_1/y_0 = \epsilon\exp\left[-\frac{f\epsilon}{f-(1-\epsilon)}\left(\frac{t}{\theta}\right)\right] + (1-\epsilon) \quad \text{for} \quad t/\theta < 1/f \qquad (5a)$$

*Tabular material has been deposited as document 5826 with the American Documentation Institute, Photoduplication Service, Library of Congress, Washington 25, D. C., and may be obtained for $1.25 for photoprints or $1.25 for 35-mm. microfilm.

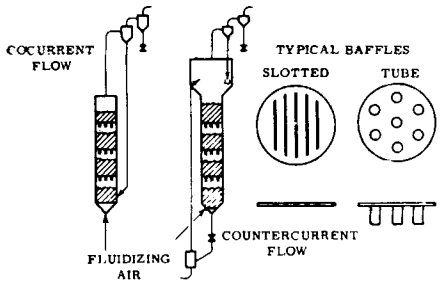

Fig. 2. Experimental apparatus.

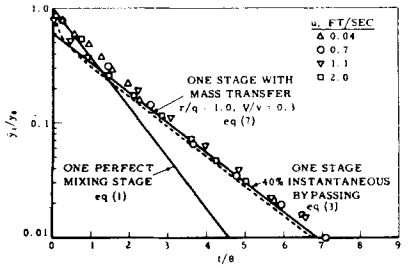

Fig. 3. Gas retention time in the unbaffled column.

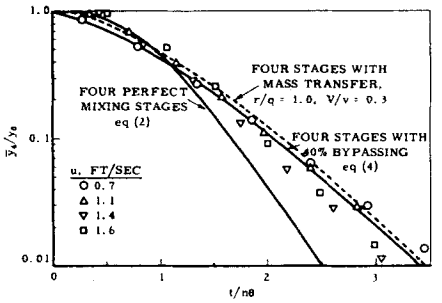

Fig. 4. Gas retention time in a compartmented column. 15% free-area grid trays, 24-in. spacing, 1/4-in. slots.

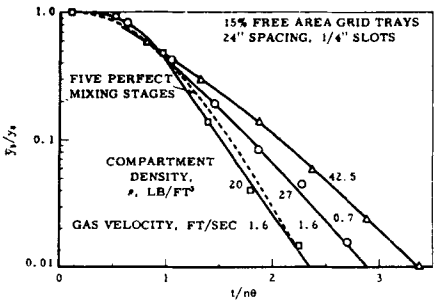

Fig. 5. Effect of compartment density on gas retention time.

$$\bar{y}_1/y_0 = \epsilon \exp\left[-\frac{f\epsilon}{f-(1-\epsilon)}\left(\frac{t}{\theta}\right)\right] \quad \text{for} \quad t/\theta > 1/f \qquad (5b)$$

where f is the ratio of by-passing velocity to superficial gas velocity.

For mass transfer between plug-flow bubbles and a single well-mixed interstitial gas phase

$$\frac{\bar{y}_b}{y_0} = \frac{1}{\left[1-\frac{r}{2q}-\frac{v}{V}\right]}\exp(-rt/V) + \left\{1-\frac{1}{\left[1-\frac{r}{2q}-\frac{v}{V}\right]}\right\}\exp(\alpha t) \quad \text{for } t < V/q \qquad (6a)$$

and

$$\frac{\bar{y}_b}{y_0} = \left[1-\frac{1}{1-\frac{r}{2q}-\frac{v}{V}}\exp(\alpha t)\right] - \left[1-\frac{1}{1-\frac{r}{2q}-\frac{v}{V}}\right]\exp(-r/q) \cdot \exp\left[\alpha\left(t-\frac{V}{q}\right)\right] \quad \text{for } t > V/q \qquad (6b)$$

where α is a zero of the following transcendental equation, in which s is the Laplace transform variable

$$s(s^2 + as + b) + c(1 - \exp[-r/q]\exp[-Vs/q]) = 0$$

and

$$a = \frac{2Vvr + V^2r}{vV^2} = \frac{r(2v+V)}{Vv}$$

$$b = \frac{r^2(V+v)}{vV^2}$$

$$c = \frac{qr^2}{vV^2}$$

For mass transfer between a well-mixed bubble phase and a well-mixed interstitial phase

$$\frac{\bar{y}_b}{y_{b0}} = \frac{\left(\frac{q}{V}+m_1\right)\exp(m_2t) - \left(\frac{q}{V}+m_2\right)\exp(m_1t)}{m_1-m_2} \qquad (7)$$

for a single stage, where

$$m_1 = -\frac{q}{2V}\left[\left\{1+\frac{r}{q}\left(1+\frac{V}{v}\right)\right\} - \sqrt{\left\{1+\frac{r}{q}\left(1+\frac{V}{v}\right)\right\}^2 - 4\frac{r}{q}\frac{V}{v}}\right]$$

$$m_2 = -\frac{q}{2V}\left[\left\{1+\frac{r}{q}\left(1+\frac{V}{v}\right)\right\} + \sqrt{\left\{1+\frac{r}{q}\left(1+\frac{V}{v}\right)\right\}^2 - 4\frac{r}{q}\frac{V}{v}}\right]$$

For the multistage case no analytic solution was made. Instead the differential equations (see supplement) were solved numerically where needed: that is, for use in Figure 4.

The model curves were next compared with the experimental retention-time curves. Since the latter contained no pronounced discontinuities for $t/\theta \leqslant 1.0$, the models for finite velocity by-passing and mass transfer into plug-flow bubbles were eliminated from further consideration. As will be shown later, the other models (perfect mixers, perfect mixers with infinite-velocity by-passing and mass transfer into well-mixed bubbles) do fit some of the experiments reasonably well. However it is quite clear that this agreement is never sufficient to show unambiguously the actual contact mechanism. When it became apparent that additional models, more plausible but of greater complexity, would contain parameters impossible to evaluate if only the effluent composition were known, model-making ceased. The experimental results were then examined in terms of the spread of gas-residence times rather than for evidence of the contact mechanism.

In the studies of steady state back-mixing of gas the concentration gradient existing upstream of the tracer injection point was used to calculate an effective diffusion coefficient. When one assumes the tracer introduced from a plane source, a homogeneous bed of solids, circular symmetry, and the absence of radial gradients,

$$D_e = \frac{uL}{\ln y_0/y} \qquad (8)$$

Over a baffle itself it is more convenient to use the concentration ratio alone as a measure of the back-mixing reduction because of the discontinuity in the concentration gradient.

It should be noted that the actual back-mixing system is much more complex than is postulated in the derivation (see supplement) of Equation (8). For example, radial gradients are not absent. In addition a plane source is only approximated by introducing the tracer downward along the column axis to impinge against a horizontal disk of a diameter about 1/4 column. Finally the tracer is back-mixing against a bulk gas flow with a velocity that varies radially from much more, to considerably less (indeed negative near the wall), than superficial. Nevertheless the effective diffusion coefficient is a convenient way of describing the back-mixing characteristics of a complex system, that is of stating the diffusivity which would be required in the ideal system postulated.

The model used for description of the solids-mixing patterns in the countercurrent flow-baffled bed considers each compartment perfectly mixed, with

TABLE 3. AVERAGE SOLIDS INTERMIXING RATES

Radioactive tracer test	Tray type	Tray, % free area	Gas velocity, ft./sec.		Average solids flow, lb./(min.)(sq. ft.) Net		Intermixing		Gross	
			U	U_r	G_c	G_r	I_c	I_r	Column	Constriction
I	Tube	4.7	0.4	8.5	0	0	9	190	9	190
II	Tube	4.7	0.4	8.5	17	350	3.5	75	20	425
	Tube	4.7	0.4	8.5	23*	480*			>23	>480
III	Tube	4.7	0.6	12.8	0	0	8.5	180	8.5	180
	Tube	4.7	0.6	12.8	12*	260*			>12	>260
IV	Tube	14.5	0.5	3.4	0	0	16.5	114	16.5	114
V	Tube	14.5	0.5	3.4	29	200	7.8	54	36.8	254
	Tube	14.5	0.5	3.4	83*	570*			>83	>570
VI	Tube	14.5	1.0	6.9	0	0	34.5	238	34.5	238
VII	Tube	14.5	1.0	6.9	29	200	29	202	58	402
VIII	Tube	14.5	1.0	6.9	58	400	26.5	183	84.5	583
	Tube	14.5	1.0	6.9	87*	600*			>87	>600
IX	Tube	14.5	1.5	10.3	0	0	39	272	39	272
	Tube	14.5	1.5	10.3	36*	250*			>36	>250

*Limiting solids downflow rates.

entrainment from the compartment below and to the compartment above and downflow from the compartment above and to the compartment below. The equations describing the transient behavior of a series of n compartments with net flow from one to n being returned to one and with intermixing are

First compartment

$$m_1 \frac{dC_1}{dt} = WC_n + w_2C_2 - (W + w_2)C_1 \qquad (9)$$

Intermediate compartments

$$m_i \frac{dC_i}{dt} = (W + w_i)C_{i-1} + (w_{i+1})C_{i+1} - (W + w_i + w_{i+1})C_i \qquad (10)$$

End compartment

$$m_n \frac{dC_n}{dt} = (W + w_n)(C_{n-1} - C_n) \qquad (11)$$

The individual intermixing rates may be determined by injecting a pulse of tracer into one of the compartments, following the change in tracer concentration with respect to time in all the compartments, and by solving Equations (9) to (11). The solution of these equations was obtained by numerical procedures or with an analogue computer.

GAS RESIDENCE-TIME DISTRIBUTION

In these experiments the bed was first fluidized with air containing about 5% helium. The flow of helium was then cut off, and the composition of the effluent from the fluid bed was determined as a function of time. Typical residence-time curves are shown in Figures 3, 4, and 5. Figure 3 represents the results for the unbaffled bed and Figure 4 for the bed compartmented by 15%-free-area slotted baffles spaced at 2-ft. intervals. The same compartmented bed is shown in Figure 5 with compartment density as parameter. The experimental data are compared with the calculated curves for three of the models discussed in the previous section: (1) perfect mixers, (2) perfect mixers with instantaneous gas by-passing, and (3) mass transfer between interstitial and bubble phases, each one perfectly mixed. The particular values of the parameters shown in Figures 3 and 4 are those which give about the best fit with the experimental results. In the single-stage case (Figure 3) the effect of by-pass fractions can easily be seen. The curve for 40% by-passing is shown, as is zero by-passing [the curve for Equation (1)]. For the case of by-pass fraction equals 0.7 the curve would decline from $\bar{y}/y_0 = 0.3$ at $t/\theta = 0$ to 0.020 at $t/\theta = 9.0$, an indication of a much slower purging rate than obtained experimentally.

The results in Figures 3 and 4 demonstrate that

1. The residence-time spectrum is considerably narrowed by the use of baffles but usually not to the extent corresponding to perfect mixers.
2. None of the models fit the experimental data with sufficient precision to indicate complete agreement with the postulated contact mechanism.
3. In the unbaffled bed the effect of gas velocity on the spectrum is insignificant in the range 0.05 to 2.0 ft./sec.

Figure 5 shows that compartment density has an effect on the residence-time distribution. The spectrum is narrowed by decreasing the compartment density either by increasing the gas velocity or decreasing the solids upflow rate. The approach to perfectly mixed compartments apparently results from the increase of the ratio of mixing energy to mass of solids within the compartment. It is not unique to the data shown but is supported by other results with the

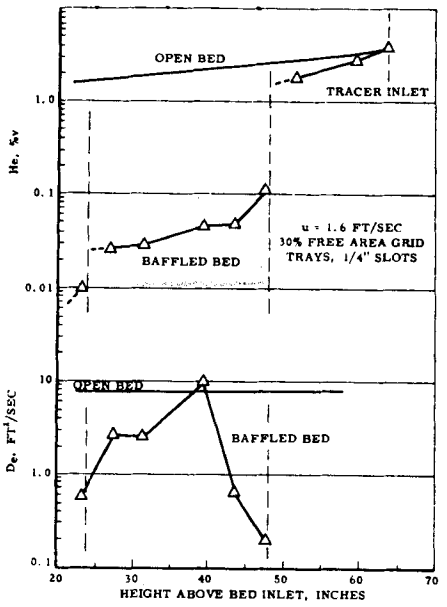

Fig. 6. The effect of baffles on gas back-mixing.

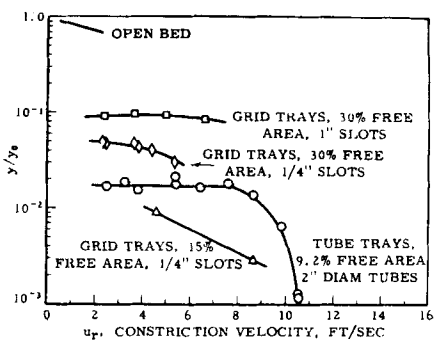

Fig. 7. Gas back-mixing as a function of slot velocity. Concentration ratio over 12 in. interval (including baffle).

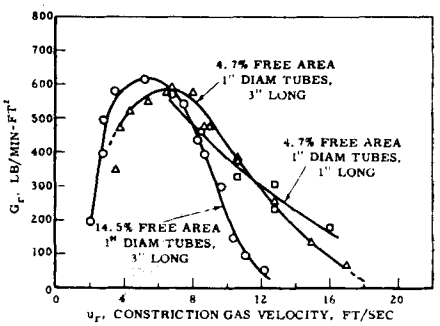

Fig. 8. Limiting solids downflow through tube trays.

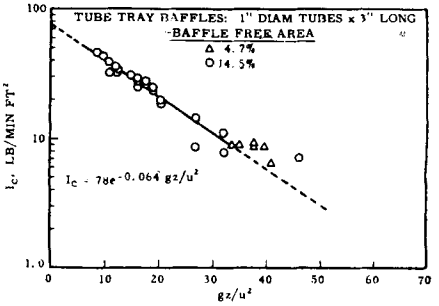

Fig. 9. Correlation of intermixing between compartments—countercurrent flow.

same baffles and higher free-area baffles. One concludes therefore that while the mass transfer and by-passing models do not correspond to the contact mechanism within the fluid bed, the residence-time spectrum can be narrowed by the use of baffles to approach, under some conditions, perfectly mixed stages.

In addition to the results reported here, other experiments were made by using slotted baffles of 30% free area and tube baffles of 2.5 to 10% free area. These results do not alter the foregoing conclusions but indicate that the 15% slotted tray may be near the best design from the standpoint of residence-time distribution and allowable velocities.

In most of the gas residence-time measurements the tracer displaced from the bed, as determined by integration of the retention-time curve, was usually about 10% greater than that calculated to be present at zero time. This is evident in Figures 1, 3, and 4 in that the experimental points usually lie to the right of the calculated curves; the cause of this phenomenon was not determined.

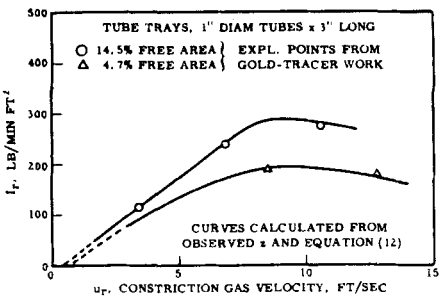

Fig. 10. Solids intermixing, zero net-solids flow.

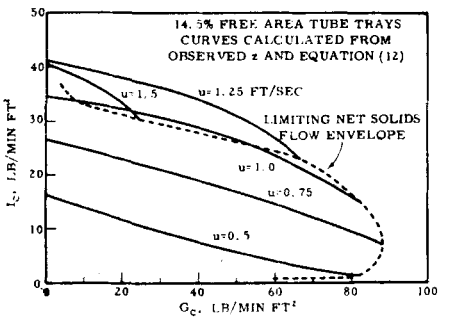

Fig. 11. Effect of solids net flow on intermixing.

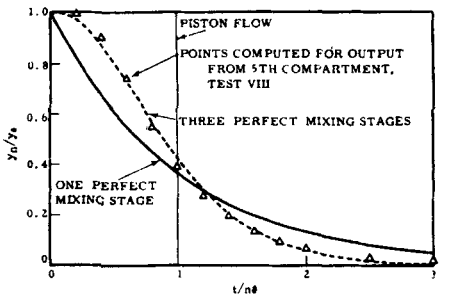

Fig. 12. Distribution of solids residence times, 14.5% free-area tube trays.

GAS BACK-MIXING

In the steady-state-gas backmixing runs gas samples were withdrawn at a low flow rate for long time periods, and so the samples were more likely to represent the interstitial volume rather than the rapidly moving bubbles. Results of typical runs are shown in Figures 6 and 7. Figure 6 shows that the concentration of helium tracer is relatively uniform throughout the unbaffled bed and within a compartment but that the concentration drops sharply across the baffles. This suggests that the solids mix freely in unbaffled regions but that their flow through the baffle is impeded. The magnitude of the latter effect will be shown in a later section. For the 16-in. unbaffled column typical values of the effective gas-diffusion coefficient are 3 to 6 sq. ft./sec., which corresponds to a Peclet number (uL/D_e) of 1 to 2 when bed length is 6 ft. The coefficients increase with velocity but not proportionally; therefore the Peclet number increases with increasing velocity.

Figure 7 shows the concentration ratio over a 1-ft. interval as a function of gas velocity through the baffle opening. It is evident that the flow of interstitial gas through the baffle becomes nil at restriction velocities of 6 to 10 ft./sec.

SOLIDS RESIDENCE TIME

In most fluid-bed processes there is a net flow of solids through the process vessel. In addition to this net flow, secondary flow patterns arise from the action of the bubbles. In the compartmented bed, solids are entrained by the rising gas into the next higher compartment; solids also flow down by gravity into the next lower compartment. In the authors' system of designation the net flow of solids is the difference between the gross flow in the same direction and a back flow (called *intermixing*) in the opposite direction. In concurrent operation reported here entrainment between the compartments is the gross flow, and the entrainment out the top of the column is the net flow; in countercurrent operation the entrainment between compartments is the intermixing flow. For the case of zero net flow the gross and intermixing flows are of course equal.

In much of this study (the work on gas residence time, compartment density, and entrainment at the top of the column) the column operated with a small net upflow resulting from the external entrainment being returned to the base of the column. For this condition the residence-time distribution and intermixing rate of solids were not determined. For countercurrent operation, however, solids net-flow rate, intermixing rates, and residence-time spectra were studied in some detail. Although both grid and tube trays were used in the concurrent studies, the countercurrent experiments were done exclusively in tube-tray baffles, because of the need for low-area baffles demonstrated by the early study and the fabrication advantage of the tube tray in cases of low free area.

The limiting solids net-flow rates in countercurrent operation were determined as a function of gas velocity by slowly increasing the withdrawal rate until a steady level could no longer be maintained in the lower compartments. These results are summarized for 4.7 and 14.5% free-area tube trays in Figure 8. The maximum solids downflow rate occurs at 4 to 7 ft./sec. constriction velocity. Lower velocities apparently result in a loss in catalyst fluidity; higher velocities load the openings with entrained solids, thus lowering the downflow rate.

The solids intermixing rate in countercurrent flow was determined by use of a radioactive tracer. A pulse of 20 g. of equilibrium catalyst, tagged with gold-198, was injected into the middle of the five-compartment bed, and the change of radioactivity concentration with time was followed in all compartments (by sample withdrawal at 15-sec. intervals). Gold-198 is a β and γ emitter with a half-life of 2.7 days. Its use permitted several experiments in a relatively short time without raising the background radioactivity of the catalyst inordinately. Lack of long-term contamination allowed continued use of the inventory catalyst. Samples were counted in a well type of scintillation counter described elsewhere (*6*).

In the first runs multiple samples were taken from each compartment. When these were found to be identical because of the intense mixing action, subsequent tests were made on the basis of one sample per compartment.

The amount of solids internal recycle was determined by solving the set of simultaneous differential Equations (9) to (11), which describes the transient change of radioacitvity concentration in each of the compartments. The best solutions, obtained on a Goodyear Electronic Data Analyzer analogue computer, indicated a different degree of solids intermixing between stages, with a greater exchange across the upper baffles. It is believed that momentary fluctuations in inventory can readily occur in the upper compartments, since the solids level in the top compartment is not constrained but that these same fluctuations are severely dampened in the lower compartments. Average values for the interchange rates are indicated in Table 3. On the basis of the individual intermixing rates and the observed dilute zone heights existing under each baffle the following correlation was developed:

$$I_c = 78e^{-0.064gz/u^2} \quad (12)$$

This correlation, shown in Figure 9, is comparable in form to entrainment correlations arising with other types of baffles.

This correlation was then used to estimate the solids intermixing rates from the observed dilute zone heights at other gas- and net-solids-flow conditions. The data and calculated curves are shown in Figures 10 and 11. Figure 10 illustrates the degree of intermixing at no net solids flow; figure 11 shows the calculated effect of net-solids flow rate on intermixing, with superficial gas velocity as parameter. Apparently intermixing increases almost linearly with increasing gas velocity until the higher gas rate limits the solids downflow and consequently the entrainment. The correlation for intermixing presented in Equation (12) is not necessarily valid for other systems, and its usefulness is limited in

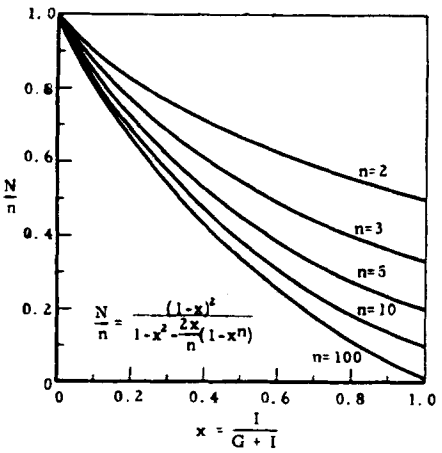

Fig. 13. Relation between number of stages and degree of intermixing.

that the dilute zone height cannot be determined accurately. However use of the Froude number may be helpful as a correlating parameter for extending meager data for some other system.

The distribution function for solids residence times may be calculated from the analogue solutions of the gold-tracer experiments or generated directly on the analogue computer. An example of the staging that can be accomplished despite the solids intermixing is depicted in Figure 12. The points shown are the calculated values of C_n following a step function change in C_1 by using Equations (9) through (11), with individual W_i's from test VIII, and setting $WC_n = 0$ in Equation (9). The curves shown are for one, three, and infinite theoretical stages.

For the general case of the reduction in staging due to intermixing, it is convenient to refer to a plot prepared by van der Laan (7) and reproduced here as Figure 13. This plot shows the relation between n actual compartments with back-mixing and the equivalent number of perfect mixers for various conditions of net and intermixing flows. In the construction of this relationship the two cases are examined in terms of the variance in the solids residence-time distribution. The required Laplace transformations are handled in the same manner as this author's treatment of longitudinal mixing in various flow regimes (8). The resulting equation is

$$\frac{N}{n} = \frac{(1-x)^2}{1 - x^2 - \frac{2x}{n}(1-x^n)} \quad (13)$$

where

$$x = I/(G+I)$$

In the case of test VIII

$$x = \frac{I}{G+I} = \frac{26.5}{58+26.5} = 0.314$$

For $n = 5$ compartments $N/n = 0.6$ from Figure 13, or $N = 3$. This close

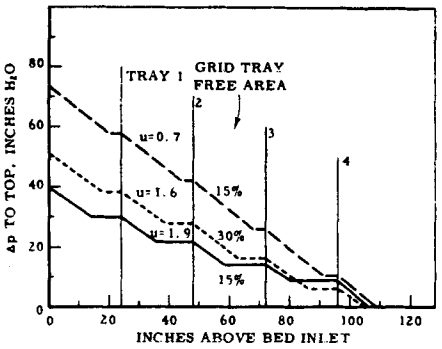

Fig. 14. Pressure profiles in compartmented bed.

agreement is indicated in Figure 12 between the calculated data and theoretical curve for three perfect-mixing stages. Thus a knowledge of the degree of solids intermixing permits determination of the number of compartments required to assure a given number of mixing stages. If the net solids downflow rate is low, a baffle design must be selected which will keep intermixing (entrainment) to a minimum.

OTHER STAGED-BED PHENOMENA

In the course of obtaining these data other characteristics of a staged fluid bed were observed. Installation of a baffle causes the formation of a dilute zone, the height of which is determined by the dynamic balance between solids downflow and solids entrainment. The presence of the dilute zone thus lowers the over-all compartment density. A detailed discussion of the effects of baffles on entrainment and compartment density follows.

Fluid-Bed Density

The fluidized bed is composed of a bubble phase of low catalyst density and a dense or interstitial phase, where density is about equal to that of the bed at incipient fluidization. As the gas velocity increases, the volume ratio of bubble phase to dense phase increases, and so the average bed density decreases. Measurements in the 16-in. column for bed heights of about 6 ft. and gas velocities of 0.01 to 3 ft./sec. show that average bed density obeys the relationship

$$\rho = 53.5 - 4.2u \text{ lb./cu. ft.} \quad (14)$$

This relation is based on the mass of solids within the bed and the height of the dense bed estimated visually or from pressure profiles.

When baffles are present in a fluid bed, the system is complicated by the appearance of dilute zones under the trays. Figure 14 shows typical pressure profiles and the existence of dilute zones in a compartmented bed. These profiles represent the axial gradient of pressure measurements at the column wall. Since the pressure drop over a length of bed

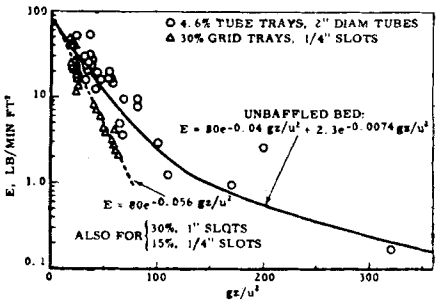

Fig. 15. Effect of baffles on solids entrainment with exit gas.

is equal to the weight of catalyst suspended, the slopes of the pressure profile are equivalent to bed density. The average density in the compartmented bed depends on the relative heights of dense and dilute zones and the density of the former. The dense-phase density probably changes with velocity in about the same manner as in the unbaffled column. The height of the dilute zone is fixed by the entrainment equation (12) for the entrainment rate and gas velocity prevailing. Thus this height will be a function of net-solids flow rate only if the net flow is large with respect to the entrainment. In most of the concurrent work the net flow rate was probably much smaller than the entrainment between compartments. Consequently, except in the case of low free-area trays, solids net-flow rate has little effect on compartment density. Equations for the average over-all compartment density as a function of superficial gas velocity at small, concurrent solids flow rates are listed in Table 4. For high, concurrent solids flow rates the densities will be higher than, and for countercurrent flow of solids the densities will be slightly lower than, those indicated by Table 4.

The effect of tray spacing was not studied in detail. From visual observa-

Table 4. Compartment Density, with Grid Baffles

Free area, %	Baffle Slot width, in.	Baffle spacing, in.	Baffle Thickness, in.	Average compartment density, lb./cu. ft.
				$\rho =$
30	1	24	⅛	$53.5 - 12u$
30	1	24	1	$53.5 - 13u$
30	¼	24	⅛	$53.5 - 16u$
30	¼	8	⅛	$53.5 - 23u$
15	¼	24	⅛	$53.5 - 18u$

tion it is concluded that the dilute zone existing at any other tray spacing will vary between a constant height and a constant percentage of the tray spacing at the same gas velocity. In Figure 14, which is for concurrent flow, it is apparent that the dilute zone height is greater under the top tray than under the lower trays. With countercurrent flow the opposite was observed; that is, the greatest dilute zone height was under the lowest tray, a situation consistent with the intermixing rates determined in the gold-tracer test. Size classification of solids was detectable only with the 2.4% free-area trays and then only to the extent of a several-micron difference in average size between adjacent compartments.

Solids Entrainment with Exit Gas

Solids entrainment into the 3-in. exit line was measured as a function of disengaging height and superficial gas velocities up to 2 ft./sec. In these measurements the disengaging section was the same diameter (16 in.) as the column, and the solids entrainment rate was estimated from the pressure drop in the calibrated exit-line nozzle. As shown in Figure 15, the rate of entrainment is either reduced or unaffected by the baffles, depending on the local velocities produced. In the unbaffled bed there is a tendency for the gas to flow at a high velocity up the center of the column rather than uniformly over the cross section. The 15 and 30% free-area baffles lower entrainment by distributing the gas flow over the column cross section. With the low free-area (2.5 to 10%) tube trays the gas flow is redistributed but into jets of high entraining power.

This comparison of baffled and unbaffled operation was made at short disengaging heights (2 to 5 ft.), where entrainment is correlated by equations similar to Equation (12). Larger disengaging heights (up to 8 ft.) were tested in the unbaffled column; in this region, as the decline of entrainment with height is less rapid, two exponential terms are required for empirical correlation of the data. At the greater heights (15 to 30 ft.) used in commercial catalytic-cracking units catalyst density has been determined by others using gamma-ray attenuation. These data indicate entrainments an order of magnitude larger than the entrainment predicted by the 16-in. open-bed correlation. The increased entrainment in the commercial units may be due partly to the very high local velocities resulting from gas maldistribution in large beds.

DISCUSSION AND CONCLUSIONS

The data discussed here are typical of the information which one must obtain to assess the potentialities of baffled fluidized beds for specific process applications. Thus one must have information on the residence-time distribution, allowable velocities, entrainment rate, and mixture density as a function of baffle design, in order to estimate the most suitable vessel configuration. Additionally one should know the chemical kinetics and the mass and heat transfer rates between gas and catalyst, if pilot-scale process data are not available.

The results presented herein demonstrate that

1. Because extensive solids and gas mixing occur in unbaffled fluidized beds, the residence-time distributions approximate a well-mixed stage. The spread in residence times may be effectively narrowed by the use of baffles, although not to the extent corresponding to an equivalent number of perfect-mixing stages in series.
2. A zone of low catalyst density appears under the baffles which lowers the over-all density in the compartment and limits the closeness of baffle spacing.
3. Solids downflow through the baffle is a function of gas velocity through the restriction and is a maximum at gas velocities of 5 to 7 ft./sec. for this system.
4. Solids entrainment between compartments and from the top of the bed is exponentially related to the Froude group. Under some conditions entrainment from the top of the bed is reduced by the presence of baffles.

ACKNOWLEDGMENT

The authors wish to acknowledge the contributions of A. E. Handlos, R. W. Kunstman, Mrs. D. K. Lidtke, M. E Stromsmoe, and J. J. Sutfin.

NOTATION

C = tracer concentration of solids, counts/(min.)(lb.)
D_e = effective diffusion coefficient, length²/time
E = entrainment rate, mass velocity, lb./(min.)(sq. ft.)
f = parameter in Equation (5*a*, *b*)
G = net-solids feed rate, mass velocity, lb./(min.)(sq. ft.)
g = acceleration of gravity, ft./sec.²
I = solids intermixing mass velocity between compartments, lb./(min.)(sq. ft.)
L = distance between sample points (where the radial average concentrations y_0 and y are measured), bed length, ft.
m = mass of solids contained in compartment, lb.
N = number of perfect-mixing stages (no intermixing or by-passing)
n = number of compartments
p = pressure, in. of water
q = volumetric gas feed rate, cu. ft./sec.
r = volumetric transfer rate of gas between bubble and interstitial phase, cu. ft./sec. of flow in (or out) of each well-mixed interstitial phase
t = time
u = superficial gas velocity, ft./sec.
u^2/gz = Froude number based on the superficial gas velocity
V = volume of bubble phase, cu. ft.
v = volume of interstitial gas phase, cu. ft.
W = solids net mass feed rate, lb./min.
w = solids intermixing mass flow rate, lb./min.
x = $I/(G + I)$
y = tracer gas mole fraction
z = solids disengaging distance above dense bed, ft., dilute zone height in a compartment

Greek Letters

ϵ = fraction of gas not by-passing
θ = residence time per stage
ρ = density of gas-solids mixtures, lb./cu. ft.

Subscripts

1, 2, 3 = sequence of stages
0 = initial or reference value
b = bubble phase
c = column cross-sectional area
g = gas
n = n^{th} stage
r = constriction (open area of baffle)

Superscripts

— = average value

LITERATURE CITED

1. Baron, Thomas, and R. A. Mugele, unpublished paper.
2. Gilliland, E. R., and E. A. Mason, *Ind. Eng. Chem.*, **44**, 218 (1952).
3. ———, and R. C. Oliver, *ibid.*, **45**, 1177 (1953).
4. Handlos, A. E., R. W. Kunstman, and D. O. Schissler, *ibid.*, **49**, 25 (1957).
5. Singer, Emanuel, D. B. Todd, and V. P. Guinn, *ibid.*, **49**, 11 (1957).
6. Todd, D. B., and W. B. Wilson, *ibid.*, **49**, 20 (1957).
7. Van der Laan, E. T., Koninklijke/Shell Laboratorium, Amsterdam, private communication.
8. ———, *Chem. Eng. Sci.*, **7**, 187 (1958).

Manuscript received December 11, 1957; revision received May 29, 1958; paper accepted June 3, 1958. Paper presented at A.I.Ch.E. Chicago meeting.